Wheat Germ Translation Initiation Factor eIF4B Affects eIF4A and eIFiso4F Helicase Activity by Increasing the ATP Binding Affinity of eIF4A†

Xiping Bi, Jianhua Ren, and Dixie J. Goss*

Department of Chemistry, Hunter College and the Graduate Center, City University of New York, 695 Park Avenue, New York, New York 10021

Received October 5, 1999; Revised Manuscript Received February 25, 2000

ABSTRACT: It has been proposed that, during translational initiation, structures in the 5′ untranslated region of mRNA are unwound. eIF4A, a member of the DEAD box family of proteins (those that contain a DEAD amino acid sequence), separately or in conjunction with other eukaryotic initiation factors, utilizes the energy from ATP hydrolysis to unwind these structures. As a step in defining the mechanism of helicase activity in the wheat germ protein synthesis system, we have utilized direct fluorescence measurements, ATPase assays, and helicase assays. The RNA duplex unwinding activity of wheat germ eIF4A is similar to other mammalian systems; however, eIF4F or eIFiso4F is required, probably because of the low binding affinity of wheat germ eIF4A for mRNA. Direct ATP binding measurements showed that eIF4A had a higher binding affinity for ADP than ATP, resulting in a limited hydrolysis and procession along the RNA in the helicase assay. The addition of eIF4B resulted in a change in binding affinity for ATP, increasing it almost 10-fold while the ADP binding affinity was approximately the same. The data presented in this paper suggest that eIF4F or eIFiso4F acts to position the eIF4A and stabilize the interaction with mRNA. ATP produces a conformational change which allows a limited unwinding of the RNA duplex. The binding of eIF4B either prior to or after hydrolysis allows for increased affinity for ATP and for the cycle of conformational changes to proceed, resulting in further unwinding and processive movement along the mRNA.

In eukaryotic translation initiation, the binding of 40S ribosome to mRNA is a complex process that requires the cooperation of at least three eukaryotic translation initiation factors, eIF4A, eIF4B, and eIF4F,[1] and the energy derived from the hydrolysis of ATP catalyzed by eIF4A and/or eIF4F (*1, 2*). Mammalian eIF4A is a 46 kDa protein that exhibits single-strand RNA-dependent ATPase activity (*3, 4*) and, in conjunction with eIF4B, double-strand RNA helicase activity (*5, 6*). Mammalian eIF4B is a 80 kDa RNA-binding protein (*1, 2* and references therein). It has been suggested that eIF4B recognizes preferentially the junction region of single- and double-strand RNA (*7*). Mammalian eIF4B also promotes the ATPase activity of eIF4A and eIF4F (*3, 4*). Mammalian eIF4A is a subunit of purified eIF4F and interacts strongly with the 220 kDa subunit of eIF4F, known as eIF4G (*1, 2* and references therein).

The eIF4A and eIF4B purified from wheat germ function similar to mammalian eIF4A and eIF4B; however, they also have some properties different from their mammalian counterparts. Unlike mammalian eIF4A which requires RNA for ATP hydrolysis, wheat germ eIF4A, a 45 kDa polypeptide, exhibits an RNA-independent ATPase activity (*8, 9*). Wheat germ eIF4B is a 59 kDa RNA-binding protein, smaller than the 80 kDa mammalian eIF4B. Similar to the function of mammalian eIF4B, the wheat germ protein promotes the ATPase activity and RNA-unwinding activity of eIF4A (*10*). Wheat germ eIF4A was found functionally equivalent to mammalian eIF4A and able to substitute for mammalian eIF4A in translation (*11*−*13*). eIF4F was also found functionally and physically similar with mammalian eIF4F except that it lacks an eIF4A-like subunit (*13, 14*). An isoenzyme, eIFiso4F, of wheat germ eIF4F was also found (*13, 14*). Its 28 kDa subunit specially binds to the 5′ cap of mRNA. In this respect, it is analogous to the 26 kDa subunit of wheat germ eIF4F (*15*−*18*). Fluorescence studies of eIFiso4F and eIF4A showed that eIFiso4F formed a complex with eIF4A and the complex bound to the cap of mRNA (*19*). Other investigations showed that eIFiso4F could catalyze the RNA-dependent ATPase activity of eIF4A (*9, 16*). Functionally, eIFiso4F is very similar to eIF4F even though these two proteins are antigenically distinct proteins (*14*). Wheat germ eIFiso4F was found able to substitute for eIF4F in translation, and the presence of both eIF4F and eIFiso4F was unnecessary (*14, 17*). eIF4A belongs to the DEAD box family of proteins, which share nine highly conserved regions (*20, 21*) and are implicated in disparate cellular processes, such as RNA splicing, translation, ribosome biogenesis, and RNA degradation (*21*). The DEAD box family of proteins share

† This work is supported by a grant from the National Science Foundation (MCB-9722907). Research Center in Minority Institution Award RR-03037 from the National Center for Research Resources of NIH supports the infrastructure at Hunter College CUNY and is also acknowledged.

* To whom correspondence should be addressed. Tel.: 212-772-5383. Fax: 212-772-5332. E-mail: dgoss@hejira.hunter.cuny.edu.

[1] Abbreviations: eIF, eukaryotic translation initiation factor; m^7G, 7-methylguanosine; TNP, trinitrophenol; AMP-PNP, 5′-adenylylimidodiphosphate; Tris, tris(hydroxymethyl)aminomethane; DTT, dithiothreitol; EDTA, ethylenediaminetetraacetic acid; HEPES, 4-(2-hydroxyethyl)-1-piperazineethanesulfonic acid.

10.1021/bi992322p CCC: $19.00
Published on Web 04/13/2000

sequence similarity with DNA helicases (*22, 23*). In addition to eIF4A, some DEAD box and related DEAH and DEXH families demonstrated an RNA helicase activity dependent on the hydrolysis of ATP (*24, 25*). Although genetic analysis has provided much information about the cellular events where the DEAD family of proteins are involved, little is known about the mechanism of action of the DEAD family of proteins at a molecular level. Mutagenesis studies of mammalian eIF4A have shown that the ATPase region (DEAD), the helicase region, and the RNA binding region in the protein have correlated functions (*26*). Recent study indicates the ATP binding and hydrolysis may produce a cycle of conformational changes in mammalian eIF4A (*27, 28*). Such a cycle of conformational changes may be used by DEAD box proteins to transduce the energy derived from ATP hydrolysis into physical work.

The RNA helicase activity of eIF4A is coupled with its ATPase activity. In this report, helicase reactions, ATPase assay, and ADP/ATP binding properties of eIF4A are reported to compare the wheat germ protein to the mammalian eIF4A and to elucidate the mechanism of helicase activity. Evidence is presented that the wheat germ eIF4A behaves in much the same manner as those characterized from the mammalian species. In addition, the ATP/ADP binding affinities of eIF4A are examined and a mechanism is proposed for the effect of eIFiso4F and eIF4B on helicase activity.

EXPERIMENTAL PROCEDURES

Reagents were purchased from the following suppliers: TNP-ADP and TNP-ATP were from Molecular Probes Inc. (Eugene, OR), AMP-PNP was from Sigma Chemical Co. [γ-^{32}P]ATP was from NEN (Boston, MA). T7 RNA polymerase, T7 primer, and nucleotides were purchased from Pharmacia Biotech. Other reagents were from Sigma, molecular biology grade (RNase, DNase, and protease free).

Purification of eIF4A, eIF4B and eIFiso4F. Wheat germ translational initiation factors eIF4A and eIFiso4F were purified according to Lax et al. (*9, 13*) and modified by Carberry et al. (*32*), eIF4B was purified according to Browning et al. (*33*). Wheat germ cDNAs for eIF4A and eIF4B were also expressed in *Escherichia coli* (BL21(DE3)-pLyS) containing the pET3d or pET23d (for eIF4A) vector in as described elsewhere (*34*). A HiTrap SP column from Pharmacia was used to purify eIF4B, and eIF4A was purified by using His-Bind kit protocal from Novagen as described therein (*35*). The protein was >95% pure for eIF4A and was about 90% pure for eIF4B as estimated by 10% SDS polyacrylamide gel electrophoresis with Commasie Brilliant Blue staining. The concentrations of protein were determined by a Bradford assay with bovine serum albumin as standard (*36*) or by using a BioRad protein assay (*37*).

Oligonucleotides. DNA templates were synthesized in an Applied Biosystems DNA synthesizer and purified by Applied Biosystems OPC column according to the protocol supplied by the manufacturer. RNAs were prepared by runoff transcription reactions of DNA templates in vitro with T7 RNA polymerase according to Milligan (*38*). 5′ capped RNA was transcribed according to Darzynkiewicz et al. (*39*) by including m^{7}GpppG in the reaction mixture. After transcription, RNAs were purified according to Daryznkiewicz et al. (*39*) by DNase 1 digestion, phenol/chloroform extraction, chloroform extraction, ethanol precipitation, and then dialysis. Products were analyzed on a polyacrylamide gel and stained by the silver staining method (*40*−*42*).

Partially double-stranded RNA duplexes were prepared by mixing equimolar amounts of each transcript in annealing buffer (40 mM HEPES, pH 7.0, 2 mM EDTA, 500 mM NaCl) and heating the mixture to 85−90 °C for 3−5 min, following by lowering the temperature to 60 °C, allowing it to slowly cool to 37 °C, and then incubating overnight at 30−37 °C. The sample was dialyzed against the helicase buffer.

Oligonucleotides used for the helicase assay were prepared as described above. RNA A and RNA B formed a partial double-stranded RNA flanked by a single stranded region of 20 nucleotides with or without an m^{7}G cap as indicated. The sequence of the RNAs is given below:

5′-m^{7}GpppGGGACCAUGGAACAACAUUAUCGCUGCGCUGCCCC 3′ B

3′ GCGACGCGACGGGG 5′ A

To determine the effects of a single-stranded region on the helicase assay, RNA C was made by transcription. This RNA was the complete compliment to RNA B, starting with the second G of the cap structure.

Helicase Assay. For the RNA helicase assay, a typical reaction mixture (10 μL) contained 20 mM Tris-HCl (pH 7.6), 70 mM KCl, 1−2 mM DTT, 2 mM ATP or as indicated, 1 mM MgOAc or as indicated, 5−10 units of RNasin (RNA guard), 2−4 ng of dsRNA substrate, and initiation factors as indicated. After 15−20 min incubation at 37 °C, the reaction mixtures were chilled on ice and reactions were terminated by adding 2 μL of loading solution containing 50% glycerol, 2% SDS, 20 mM EDTA, and 0.1% bromphenol blue. The samples were loaded onto a 15% nondenaturing polyacrylamide gel and electrophoresed in TBE (tris/borate/EDTA) buffer to analyze the degree of unwinding of the duplex RNA. In all experiments, control lanes with duplex and unhybridized RNAs were run for comparison. The gel was silver stained as described above and scanned by a soft laser-scanning densitometer (Zenith) or Scanlyst scanned (Ambis). The unwinding efficiency was calculated according to the percentage of double-stranded and unwound single-stranded RNAs relative to the total input duplex RNA.

ATPase Assay. The ATPase activity of eIF4A and (eIF4A + eIF4B) was determined by measuring the release of $^{32}P_i$ as described previously (*3, 4*). The standard assay was performed in a reaction volume of 20 μL, which contained 25 mM HEPES/KOH, pH 7.5, 100 mM KCl, 2.0 mM MgAOc, 1.0 mM DTT, and 0.1 mM [γ^{32}-ATP] (total amount of ATP was 2000 pmol; 200−800 cpm/pmol was used), and indicated amount of initiation factors. For the time course of ATP hydrolysis assay, 3 μL of reaction solution was taken from the standard assay solution at indicated times. The amount of $^{32}P_i$ released was calculated according to the standard assay where the total amount of ATP was 2000 pmol. For eIF4A or eIF4B, all values were corrected for the amount of $^{32}P_i$ released in the absence of initiation factors. For the (eIF4A + eIF4B) mixture, the ATPase activity was corrected for the amount of $^{32}P_i$ released in the presence of eIF4B (4.2 pmol/(h/μg) in standard assay).

Fluorescence Titration Measurements. All fluorescence titrations were accomplished by using a Spex Fluorolog τ2 spectrofluorometer. When the Trp intrinsic fluorescence of the protein is measured, the excitation wavelength was 295 nm and emission wavelength was 345 nm. When the fluorescence of trinitrophenyl group in TNP-ADP is measured, the excitation wavelength was 408 nm and emission wavelength was 540 nm. All fluorescence intensities were corrected, when necessary, for the inner-filter effect by using the following formula (*43*):

$$F_c = (F - B)10^{0.5L(A_{ex}+A_{em})} \quad (1)$$

Here F_c is the corrected fluorescence intensity, F is the measured fluorescence intensity, B is the background of the measurements, and L is the length of optical path in the cuvette in centimeters for excitation light and emission light, respectively. A_{ex} and A_{em} are the absorbance of the sample at excitation and emission wavelengths, respectively. The dissociation constants were obtained by fitting the titration data to the following equation analogous to those given previously (*44*):

$$F = \frac{2F_0K_d - F_\infty(K_d + P_0 + L_0) + F_\infty((K_d + P_0 + L_0)^2 - 4P_0L_0)^{1/2}}{(K_d + P_0 - L_0) + ((K_d + P_0 + L_0)^2 - 4P_0L_0)^{1/2}} \quad (2)$$

Here F_0 and F_∞ are fluorescence intensities of protein and protein−ligand complex, respectively. P_0 and L_0 are the initial concentrations of protein and nucleotide, respectively. K_d is the dissociation constant of the binding reaction. Nonlinear least-squares fitting of the titration data was performed using KaleidaGraph software (Version 2.1.3, Abelbeck Software, 1991).

RESULTS

Design of Helicase Substrates. Recent reports of a mechanism of eIF4A helicase activity (*5*) have indicated that eIF4A alone is unable to unwind double-stranded RNA that has about 15 bp. To determine the details of this process, we have examined the effects of initiation factors from wheat germ on a partially double stranded RNA with 14 bp, a cap at the 5′ terminus, and a 20 base single-stranded region (oligo-cAB). This RNA contained all of the features that should be necessary for helicase activity. A similar RNA was constructed that lacked the 5′ terminal m^{7}G cap (oligo-AB) and a fully double-stranded RNA (oligo-AC) without a single-stranded region was also constructed. These oligonucleotides allow us to assess the effects of the cap group, the requirement for a single-stranded region for binding, and the effect of other initiation factors on the reactions. Since oligo-AB had all of the features necessary for measuring helicase activity, we first determined the conditions for unwinding of this RNA.

Requirements for ATP and Magnesium. eIFiso4F and eIF4A require ATP for unwinding as do all helicases described to date (*37, 45, 46*). An ATP concentration of 2.0 mM was found to be saturating (data not shown). We have previously reported that ATP was necessary for eIF4A and eIFiso4F complex formation and might also be needed for hydrogen bond disruption and for strand separation (*19*). The nonhydrolyzable ATP analogue, AMP-PNP, and other nucleoside triphosphates, GTP, UTP, and CTP, were unable to support unwinding (data not shown).

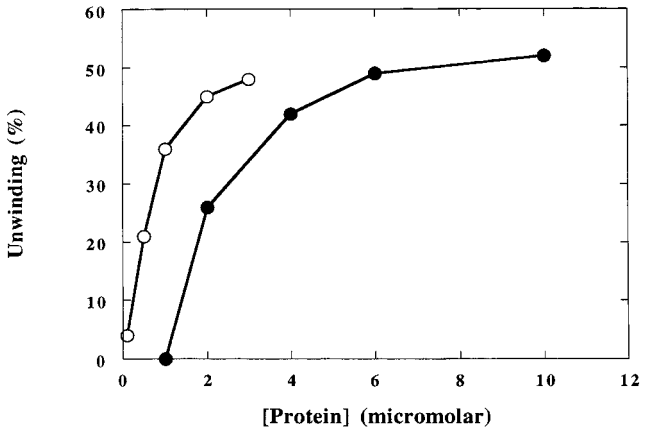

FIGURE 1: eIF4A and eIFiso4F concentration dependence of helicase reaction. The concentrations of ATP, Mg^{2+}, and eIFiso4F were 2.0 mM, 1.0 mM, and 3.3 μM, respectively. Reaction time was 15 min. For eIFiso4F (open circles), the concentrations of ATP, Mg^{2+}, and eIF4A were 2.0 mM, 1.0 mM, and 10 μM, respectively. Reaction time was 15 min.

There is an absolute requirement for magnesium in the helicase reaction. In the absence of Mg^{2+}, there is no detectable helicase activity. The maximum amount of unwinding occurs at a [Mg^{2+}] of 0.6−1.0 mM (data not shown). The time course of the unwinding reaction was also monitored which revealed a rapid increase that reached a plateau at approximately 50% unwinding in 15 min (data not shown). These experiments established conditions that allow examination of the effects of other proteins on the helicase reaction as well as measure the effects of binding of ATP and ADP.

Effects of Protein Concentration. eIF4A is a DEAD box protein and has been shown to have helicase activity (*5, 6*). However, most of these studies have required a large excess of eIF4A. Figure 1 shows the effect of increasing wheat germ eIF4A and eIFiso4F concentrations on helicase activity in the presence of a constant amount of all other materials. With increasing amounts of eIF4A, there was an increase in the amount of RNA unwound; however, this activity leveled off when approximately 50% of the duplex RNA was unwound. The low efficiency of eIF4A as a helicase is only partially accounted for by its relatively low binding affinity (*19*).

The effect of eIFiso4F concentration and the cap structure on helicase activity is also shown in Figure 1. eIFiso4F is required for the helicase reaction under these conditions. The 28 kDa subunit of eIFiso4F is a cap binding protein. The maximum unwinding was again found to be less than 100%. The fact that the optimum ratios of eIFiso4F:eIF4A are less than 1:1 can be accounted for from the equilibrium constants for RNA binding and eIFiso4F:eIF4A interaction. When the reaction was performed with the oligo-AB, which lacks the cap structure, no unwinding occurred even at increased protein concentrations (data not shown). These data support the conclusion that one role of eIFiso4F is to increase the eIF4A affinity and to locate the complex at the 5′ terminus of RNA.

The mammalian eIF4B has been shown to have a catalytic effect on the helicase reaction (*5*). Table 1 shows the effect

Table 1: Requirement of m^7G Cap in Helicase Reaction

proteins	ratio (%) dsRNA	RNA A	RNA B	unwinding (%)
	Capped RNA			
4A + iso4F	49.1	34.2	16.7	50
4A + 4B + iso4F	0	73.7	26.3	100
	Uncapped RNA			
4A + iso4F	100	0	0	0
4A + 4B + iso4F	66.6	20.5	12.9	33

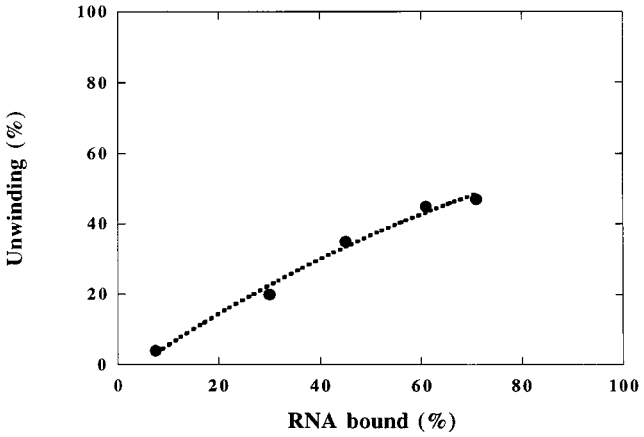

FIGURE 2: Comparison of RNA duplex binding to the initiation factor complex with RNA duplex unwinding. The percentage of RNA bound was calculated according to the equilibrium association constant determined previously (*19*). The percentage of unwinding was taken from Figure 4. The dashed line is the fitted curve of the data to a second-order polynomial equation.

of eIF4B on both capped and uncapped RNA unwinding. By addition of eIF4B, capped oligonucleotide could be fully unwound; uncapped oligonucleotide was unwound up to 33%. Since a complex of eIF4B and eIF4A binds RNA almost as well as a complex of eIFiso4F + eIF4B + eIF4A, the effects of eIFiso4F appear to be more complex than simply increasing the binding affinity. Figure 2 shows the comparison between the percentage of RNA bound to the initiation factor complex and the RNA unwound by the complex. The amount of oligonucleotide bound was calculated from the equilibrium constant determined previously (*19*). The amount of oligonucleotide unwound is from the data in Figure 1. It can be seen that even at a projected 100% binding, not all of the RNA will be unwound in the absence of eIF4B. To further elucidate the mechanism of this reaction, ATP and ADP binding studies were carried out.

eIF4A and eIF4B ATPase Assay. The time courses of ATP hydrolysis catalyzed by eIF4A and a combination of eIF4A and eIF4B are shown in Figure 3. At an ATP concentration of 100 μM, only about 20% of the ATP was hydrolyzed by eIF4A alone. This was not due to inactivation of eIF4A during the assay since the preincubation of eIF4A for 1 h at 25 °C had no effect on the time course of ATP hydrolysis. The presence of 20 μg/mL of poly(U) also had no effect on the time course of ATP hydrolysis catalyzed by eIF4A, consistent with previous observations that eIF4A has an inherent RNA-independent ATPase activity (*9*). When an equal molar amount of eIF4B was mixed with eIF4A, the hydrolysis increased to approximately 50% of the ATP (100 μM). The limited hydrolysis of ATP suggests that ADP may be a product inhibitor. To explore this possibility, we

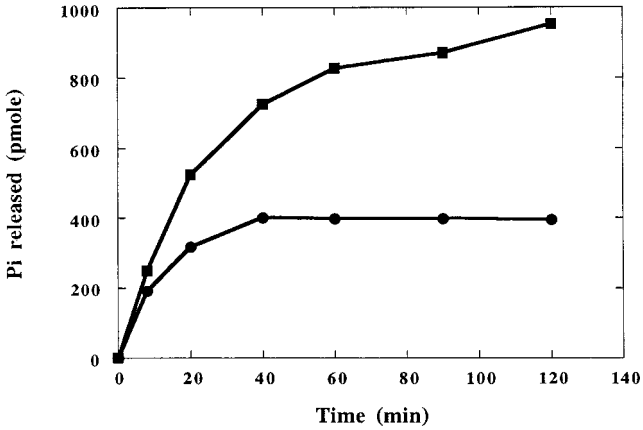

FIGURE 3: Time course of ATP hydrolysis catalyzed by eIF4A and eIF4A + eIF4B. In the standard assay solution, the concentration of ATP was 100 μM and the amounts of eIF4A and eIF4B were 6 and 10 μg, respectively. Filled circles refer to the time course of ATP hydrolysis catalyzed by eIF4A; filled squares refer to the time course of ATP hydrolysis catalyzed by eIF4A + eIF4B.

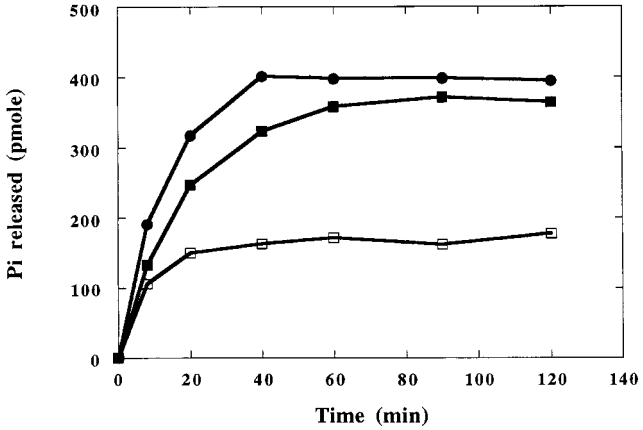

FIGURE 4: Time course of ATP hydrolysis catalyzed by eIF4A in the presence ADP and AMP-PNP. In the standard assay solution, the concentration of ATP was 100 μM and the amounts of eIF4A and eIF4B were 6 and 10 μg, respectively. The concentrations of ADP and AMP-PNP were 100 and 500 μM, respectively. Key: filled circle, eIF4A alone; open square, in the presence of 100 μM ADP; filled square, in the presence of 500 μM AMP-PNP.

performed the same assay in the presence of 100 μM ADP. In this case, about half the amount of ATP was hydrolyzed compared to the reaction in the absence of added ADP. The presence of 500 μM AMP-PNP, a nonhydrolyzable analogue of ATP, however, had only a small effect on the amount of ATP hydrolyzed (Figure 4). The hydrolysis of ATP is completely dependent on the presence of Mg^{2+}. In the absence of Mg^{2+}, the hydrolysis of ATP is completely abolished (data not shown).

Binding of TNP-ADP to eIF4A and eIF4A−eIF4B Complex. TNP-ADP is a fluorescent analogue of ADP where the ribose 2′ and 3′ oxygens are attached to a trinitrophenyl (TNP) group (*47*). The fluorescence intensity of TNP-ADP increased severalfold when bound to eIF4A with a blue shift of emission maximum from 550 nm for free probe to 538 nm for eIF4A bound probe (Figure 5a). The fluorescence properties of TNP-ADP are very sensitive to solvent polarity and suitable as a reporter of the microenvironment of the nucleotide binding site (*47*−*49*). The large increase in fluorescence intensity and the blue shift of the emission maximum of TNP-ADP upon the binding of eIF4A suggest

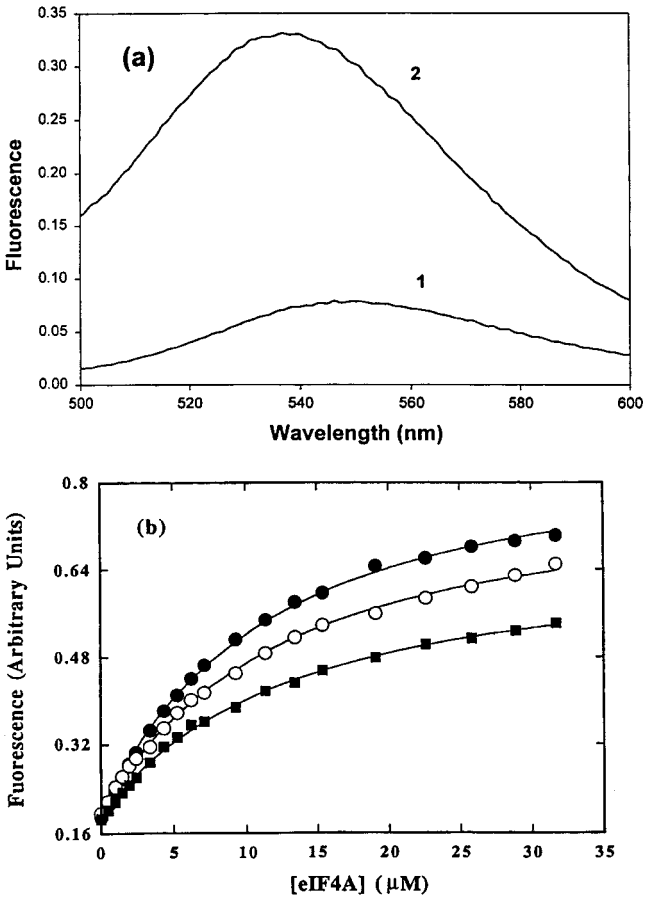

FIGURE 5: Fluorescence titrations of TNP-ADP with eIF4A and eIF4A + eIF4B monitored by the increase of the fluorescence of the TNP-ADP. The concentration of TNP-ADP was 3.68 μM. The excitation wavelength was 408 nm, and the emission wavelength was 540 nm. (a) Change of the fluorescence spectrum of TNP-ADP upon the binding of eIF4A: spectrum 1, TNP-ADP alone; spectrum 2, TNP-ADP + 31.7 μM eIF4A. (b) Titrations of TNP-ADP with eIF4A (open circle); with equal molar eIF4A and eIF4B mixture (filled circled), and with eIF4A in the presence of 50 μg/mL poly(U). The solid lines are the fitted curves to eq 2.

the ribose-binding site of ADP has a predominantly hydrophobic character (*50*). Figure 5b shows the fluorescence intensity of TNP-ADP upon the titration with eIF4A and eIF4A + eIF4B. The data were fitted to eq 2. The dissociation constant obtained from the fluorescence titration of TNP-ADP with eIF4A was 10.7 μM. The dissociation constant obtained from the fluorescence titration of TNP-ADP with eIF4A + eIF4B was 9.8 μM. In the presence of 50 μg/mL poly(U), a dissociation constant of 11.7 μM was obtained. These dissociation constants indicate that eIF4B has no substantial effect on the affinity of eIF4A for TNP-ADP. Poly(U) also has no significant effect to the affinity of eIF4A for TNP-ADP. In the absence of Mg^{2+}, the dissociation constant obtained from the fluorescence titration of TNP-ADP with eIF4A was 15.5 μM (data not shown), indicating that Mg^{2+} has a moderate effect on the affinity of eIF4A for TNP-ADP.

Fluorescence Titration of eIF4A, eIF4B, and eIF4A + eIF4B with TNP-ADP. To determine the number of TNP-ADP bound on eIF4A, eIF4B, and eIF4A + eIF4B, fluorescence titrations of eIF4A, eIF4B, and eIF4A + eIF4B with TNP-ADP were performed, as shown in Figure 6. After the inner-filter effect corrections, we observed a 30%

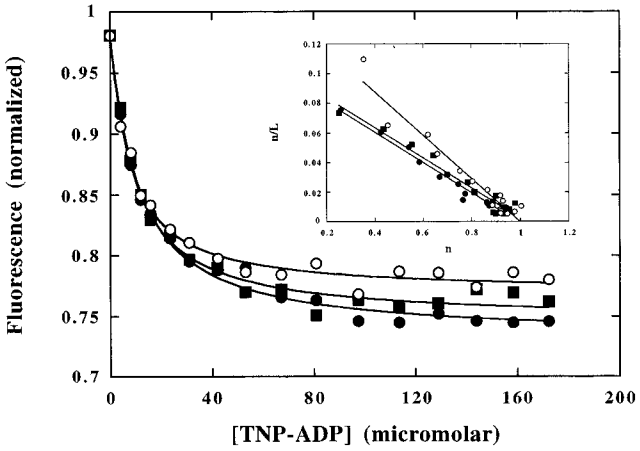

FIGURE 6: Fluorescence titrations of eIF4A, eIF4B, and complex eIF4A + eIF4B with TNP-ADP by monitoring the quenching of intrinsic Trp fluorescence of protein: eIF4A (100 μg/mL, about 2.2 μM; solid circles), eIF4B (150 μg/mL; squares); eIF4A−eIF4B complex (open circles) titrated with TNP-ADP. For the titrations, excitation wavelength was 295 nm, and emission wavelength was 345 nm. The solid lines are the fitted theoretical curves of eq 2. The insert is the corresponding Scatchard analyses of the titration data. The number of moles of TNP-ADP bound was calculated by assuming a single binding site (*56*), and then, $n = (F_0 - F)/(F_0 - F_\infty)$.

quenching of protein Trp fluorescence upon the binding of TNP-ADP. It has been suggested that the quenching of Trp fluorescence upon the binding of TNP-ADP or TNP-ATP is due to the efficient fluorescence energy transfer from the Trp to the bound TNP group of the nucleotide (*50*). A large quenching effect (76%) of Trp fluorescence of DnaB protein upon the binding of TNP-ATP has been observed, suggesting a cluster of Trp in proximity to the nucleotide binding site of DnaB protein (*50*). Since only 30% quenching of Trp fluorescence was observed in the present measurements, part of the Trp residues in eIF4A and eIF4B are located near the nucleotide binding site of the proteins and others may be more distant. The dissociation constant obtained for eIF4A titrated with TNP-ADP was 10.1 μM, that for eIF4B titrated with TNP-ADP was 7.0 μM, and that for eIF4A + eIF4B was 8.7 μM. These data are consistent with the dissociation constants obtained by titration of TNP-ADP with eIF4A and eIF4A + eIF4B. Scatchard analysis of the binding data shown in Figure 6 suggests that eIF4A, eIF4B, and eIF4A + eIF4B each bound a single TNP-ADP. It is known that eIF4B is an RNA-binding protein (*10*, *51*). Therefore, the binding of TNP-ADP to eIF4B observed in this measurement might be due to the nonspecific binding of TNP-ADP to the RNA binding site in the protein. However, the Scatchard analysis of the fluorescence titration of eIF4A + eIF4B with TNP-ADP seems to suggest that there is a specific nucleotide binding site for the complex. The binding to eIF4B may either be part of the nonspecific binding or the association of the two proteins form a single unique binding site. When eIF4A was titrated with TNP-ATP (data not shown), a dissociation constant of 19.4 μM was observed, a value about 2-fold larger than the dissociation constant of eIF4A with TNP-ADP (Table 2). It was observed that TNP-ATP is a competitive inhibitor of ATP for in vitro translation in the wheat germ system (*52*). The hydrolysis rate of TNP-ATP catalyzed by DnaB is about 100-fold lower than that of ATP (*53*), and TNP-ATP has been used in fluorescence titration

Table 2: Dissociation Constants, K_d, for ADP, AMP-PNP, TNP-ADP, and TNP-ATP Binding to eIF4A, eIF4B, and eIF4A + eIF4B, Determined by Fluorescence Titration

	K_d (μM)[a]			
proteins	ADP	AMP-PNP	TNP-ADP	TNP-ATP
eIF4A	2.8 ± 0.2	14.2 ± 1.3	10.1 ± 0.5 10.7 ± 0.4[b] 15.5 ± 0.9[b,c]	19.4 ± 0.9
eIF4B	5.7 ± 0.3	12.7 ± 0.7	7.0 ± 0.6[b]	ND
eIF4A + eIF4B	3.6 ± 0.4	1.6 ± 0.2	8.7 ± 0.6 9.8 ± 0.3[b]	ND
eIF4A + poly(U)	ND	ND	11.7 ± 0.5[b]	ND

[a] All dissociation constants were obtained by fitting the fluorescence titration data to eq 2. [b] Dissociation constants obtained by titrating TNP-ADP with eIF4A or eIF4 + eIF4B. All other K_ds were obtained by titrating protein with nucleotide. [c] In the absence of Mg^{2+}. [d] ND, not determined.

of DnaB protein. This suggests the hydrolysis of TNP-ADP catalyzed by eIF4A in the fluorescence titration measurement may be negligible. However, we were unable to measure this directly.

Direct Fluorescence Titration of eIF4A, eIF4B, and eIF4A + eIF4B with ADP and AMP-PNP. To further determine the affinities of ADP and ATP, the nonhydrolyzable ATP analogue AMP-PNP and ADP were used to titrate the protein solutions. When eIF4A, eIF4B, and eIF4A + eIF4B were titrated directly with ADP or AMP-PNP, we observed about 11% quenching of Trp fluorescence of eIF4A, 15% quenching of Trp fluorescence of eIF4B, and about 7% quenching of Trp fluorescence of eIF4A + eIF4B. These observations are consistent with the suggestion that some of the tryptophan residues of eIF4A and eIF4B are located in proximity to the nucleotide binding site of the protein. The quenching of Trp fluorescence was used to determine the dissociation constants of eIF4A, eIF4B, and eIF4A + eIF4B with ADP and AMP-PNP, by fitting the fluorescence titration data as described above. Table 2 summarizes the dissociation constants determined. A comparison of the dissociation constants gives two important conclusions. First, eIF4A has a higher affinity for ADP with a dissociation constant of 2.8 μM and a lower affinity for AMP-PNP with a dissociation constant of 14.2 μM. That is, the affinity of eIF4A for ADP is five times higher than for ATP. Second, the interaction between eIF4A and eIF4B enhances remarkably the affinity of the complex for AMP-PNP, enhancing the binding almost 9-fold (K_d changing from 14.2 to 1.6 μM). In addition, the TNP group has a substantial effect on the affinity of eIF4A for ADP, leading to about 4-fold increase of the dissociation constant (from 2.8 to 10.1 μM). However, the affinity of eIF4A for ATP is less affected by the presence of TNP group, with a change of dissociation constant from 14.2 μM for AMP-PNP to 19.4 μM for TNP-ATP.

DISCUSSION

Hydrolysis of ATP is required for the RNA helicase activity of eIF4A. It was confirmed that in absence of ATP no helicase activity occurred (*5*, *6*). The binding of ADP and ATP to eIF4A can provide valuable information about the mechanism of the coupling between ATPase activity and RNA helicase activity of eIF4A.

The ATPase assay presented in this paper demonstrated that the percentage of ATP hydrolyzed is dependent on the ratio of ADP/ATP in the assay solution. Fluorescent titration measurements showed that the binding affinity of eIF4A for ADP is 5-fold higher than for ATP, indicating that ADP is a strong product inhibitor of ATP hydrolysis catalyzed by eIF4A. For mammalian eIF4A, the affinity of eIF4A for ADP is about 10-fold higher than the affinity of eIF4A for ATP at pH 7.4 and about 80-fold higher at pH 6.0 (*27*). Lorsch and Hershlag (*27*) obtained values of K_m, which it is suggested are equal to values of K_d, of 80 μM for ATP and 1 μM for ADP. However, earlier measurements (*55*) of K_m for ATP obtained values about 4-fold lower than those of (*27*). Our values of K_d of 2.8 μM for ADP and about 15−20 μM are in good agreement with earlier measurements. These differences may be due to differences in the plant system, slight differences in the conditions, or differences between $K_{m,app}$ and K_d.

Lorsch and Herschlag (*27*) suggested that, for mammalian eIF4A, ATP binding and hydrolysis produce a cycle of conformational changes in eIF4A, and such a cycle of conformational changes may be used by eIF4A to unwind the secondary structure of RNA. Our fluorescence titration measurements demonstrate that the trinitrophenyl group has a substantial effect on the affinity of eIF4A for ADP but has only a small effect on the affinity of eIF4A for ATP (see Table 2), suggesting that the structure of the ADP binding site of eIF4A is different from the structure of the ATP binding site. These facts are consistent with a two-state model, as proposed by Lorsch and Hershlag (*27*).

We do not see a significant difference in RNA binding affinity of eIF4A in the presence of ATP. This is in agreement with the data at pH 7.0 reported by Lorsch and Herschlag (*27*). Other initiation factors play a significant role in the helicase activity. In the wheat germ system, eIF4F or eIFiso4F in addition to eIF4A is required for a significant helicase activity. Part of the effect of eIF-iso4F is to increase the RNA-binding affinity of eIF4A, which alone has a very low affinity for RNA. As shown in Figure 2, the increase in affinity alone cannot completely explain the effect of eIFiso4F. It appears likely that location of the eIF4A near the cap structure, which would be efficiently accomplished by an eIF4A/eIF4F complex, enhances the efficiently of unwinding.

In the presence of eIF4B, the amount of ATP hydrolyzed by eIF4A is increased. Fluorescence titration measurements demonstrate that the interaction between eIF4A and eIF4B increases about 8-fold the affinity of eIF4A for AMP-PNP, while the affinity for ADP is only slightly affected. eIF4B promotes the release of ADP from eIF4A by increasing the affinity of eIF4A for ATP, rather than by decreasing the affinity of eIF4A for ADP. A kinetic study on the binding of ADP or ATP to eIF4A is necessary to illustrate the mechanism of the interaction between eIF4A and eIF4B. In addition, it is interesting to compare the interactions of mammalian eIF4A, eIF4B, and RNA with those of wheat germ eIF4A, eIF4B, and RNA. For mammalian eIF4A, its affinity for ATP increases about 8-fold upon the binding of RNA at pH 6.0 (*27*), while the interaction between eIF4A and eIF4B seems primarily to increase the affinity of eIF4A for RNA (*55*). For wheat germ eIF4A, the present results demonstrate that wheat germ eIF4B functions to enhance the affinity of eIF4A for both ATP and RNA, since wheat germ eIF4B, like its mammalian counterpart, is also a strong

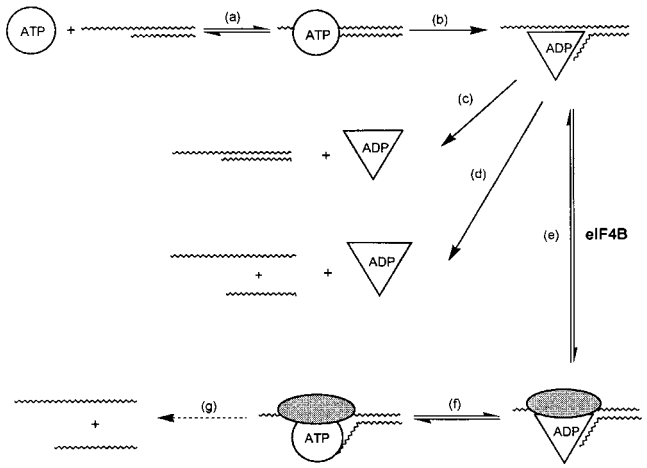

FIGURE 7: Proposed model for the RNA helicase activity of wheat germ translation initiation factor complex formed by eIF4A, eIF4B, and eIFiso4F. eIFiso4F is not shown in the picture for clarity. The circle marked with ATP refers to the eIF4A/ATP complex, the triangle marked with ADP refers to eIF4A/ADP complex, and the shadowed oval represents eIF4B, and the zigzag curve represents RNA.

RNA-binding protein (*51*). Rogers et al. (*6*) have presented evidence that shows mammalian eIF4A is a nonprocessive helicase able to unwind only a minimal number of base pairs. This was not due to lack of binding or ADP inhibition. Our results are similar in that the effects of eIF4B cannot be accounted for by an increase in RNA binding affinity since eIFiso4F will enable the eIF4A to be bound to the RNA but does not completely unwind the duplex (Table 1). In terms of the kinetic model of RNA unwinding proposed by Rogers et al. (*6*), our data would add an additional step to demonstrate the role of eIF4B, as shown in Figure 7. eIFiso4F is also present, probably complexed with eIF4A; however, we have not shown eIFiso4F separately from eIF4A in the figure for clarity. Steps a and b represent the binding of eIF4A/ATP complex to RNA and an initial partial unwinding. At this stage, the reaction follows either step (c) where the protein dissociates and the RNA reanneals or the destablized RNA continues to unwind at the thermodynamic melting rate and at some point the protein dissociates. Our model proposes that, after the first ATP hydrolysis and partial unwinding of RNA, eIF4B allows turnover of ADP for ATP (step f) and further unwinding by hydrolysis of ATP (step g). This may occur multiple times to destabilize the double-stranded RNA and promote strand separation. The exact sequence of events and kinetics of reaction rates will require more detailed analysis. Our data, however, demonstrate that the role of eIF4B is to shift the ATP/ADP binding affinity of eIF4A and provide a possible mechanism that permits the processive unwinding of RNA either by eIF4A or the eIF4A−eIF4B complex.

ACKNOWLEDGMENT

We wish to thank Dr. Karen Browning for the plasmids containing the eIF clones and globin mRNA and Ilias Triantafyllou for technical assistance and helpful discussions.

REFERENCES

1. Merrick, W. C. (1994) *Biochimie 76*, 822−830.
2. Merrick, W. C., and Hershey, J. W. B. (1996) *Translational Control*, pp 31−69, Cold Spring Harbor Laboratory, Plainview, NY.
3. Grifo, J. A., Abramson, R. D., Salter, C. A., and Merrick W. C. (1984) *J. Biol. Chem. 259*, 8648−8654.
4. Ray, B. K., Lawson, T. G., Kramer, J. C., Claderos, M. H., Grifo, J. A., Abramson, R. D., Merrick, W. C., and Thach, R. E. (1985) *J. Biol. Chem. 260*, 7651−7658.
5. Rozen, F., Edery, I., Meerovitch, K., Dever, T. E., Merrick, W. C., and Sonenberg, N. (1990) *Mol. Cell. Biol. 10*, 1134−1144.
6. Rogers, G. W., Richter, N. J., and Merrick, W. C. (1999) *J. Biol. Chem. 274*, 12236−12244.
7. Methot, N., Pause, A., Hershey, J. W. B., and Sonenberg, N. (1994) *Mol. Cell. Biol. 14*, 3207−3216.
8. Metz, A. M., and Browning, K. S. (1993) *Gene 15*, 299−300.
9. Lax, S. R., Browning, K. S., Maia, D. M., and Ravel, J. M. (1986) *J. Biol. Chem. 261*, 15632−15636.
10. Browning, K. S., Fletcher, L., Lax, S. R., and Ravel, J. M. (1989) *J. Biol. Chem. 284*, 8491−8494.
11. Abramson, R. D., Browning, K. S., Dever, T. E., Lawson, T. G., Thach, R. E., Ravel, J. M., and Merrick, W. C. (1988) *J. Biol. Chem. 263*, 5462−5467.
12. Seal, S. N., Schmidt, A., and Marcus, A. (1983) *J. Biol. Chem. 258*, 859−865.
13. Lax, S. R., Lauer, S. J., Browning, K. S., and Ravel, J. M. (1986) *Methods Enzymol. 118*, 109−128.
14. Lax, S. R., Fritz, W., Browning, K., and Ravel, J. (1985) *Proc. Natl. Acad. Sci. U.S.A. 82*, 330−333.
15. Seal, S. N., Schmidt, A., Marcus, A., Edery, I., and Sonenberg, N. (1986) *Arch. Biochem. Biophys.* 710−715.
16. Browning, K. S., Lax, S. R., and Ravel, J. M. (1987) *J. Biol. Chem. 262*, 11228−11232.
17. Lax, S. R., Fritz, W., Browning, K., and Ravel, J. (1984) *Fed. Proc. 43*, 1937.
18. Browning, K. S., Lax, S., and Ravel, J. M. (1985) *Fed. Proc. 44*, 1224
19. Balasta, M. L., Carberry, S. E., Friedland, D. E., Perez, R. A., and Goss, D. J. (1993) *J. Biol. Chem. 268*, 18599−18603.
20. Schmid, S. R., and Linder, P. (1992) *Mol. Microbiol. 6*, 283−292.
21. Wassarman, D. A., and Steitz, J. A. (1991) *Nature 349*, 463−464.
22. Koomin, E. V. (1991) *Nature 352*, 290.
23. Bork, P., and Koomin, E. V. (1993) *Nucleic Acids Res. 21*, 751−752.
24. Hirling, H., Scheffner, M., Restle, T., and Stahl, H. (1989) *Nature 339*, 562−564.
25. Lain, S., Richmann, L. J., and Garcia, J. A. (1990) *Nucleic Acids Res. 18*, 7003−7006.
26. Pause, A., Methot, N., and Sonenberg, N. (1993) *Mol. Cell. Biol. 13*, 6789−6798.
27. Lorsch, J. R., and Herschlag, D. (1998) *Biochemistry 37*, 2180−2193.
28. Lorsch, J. R., and Herschlag, D. (1998) *Biochemistry 37*, 2194−2206.
29. Jagus, R., Anderson, W. F., and Safer, B. (1981) *Prog. Nucleic Acid Res. Mol. Biol. 25*, 127−185.
30. Mathews, M. B., Sonenberg, N., and Hershey, J. W. B. (1996) *Translational Control*, pp 1−29, Cold Spring Harbor Laboratory Press, Plainview, NY.
31. Kozak, M. (1989) *J. Cell. Biol. 108*, 229−241.
32. Carberry, S. E., Darzynkiewicz, E., and Goss, D. J. (1991) *Biochemistry 30*, 1624−1627.
33. Browning, K. S., Maia, D. W., Lax, S. R., and Ravel, J. M. (1987) *J. Biol. Chem. 262*, 538−541.
34. Browning, K. S. (personal comunication).
35. Bi, X., and Goss, D. J. (manuscript in preparation).
36. Bradford, M. M. (1976) *Anal. Biochem. 72*, 248−254.
37. Lahaye, A., Leterme, S., and Foury, F. (1993) *J. Biol. Chem. 268*, 26155−26161.
38. Milligan, J. F., Groebe, D. R., Witherell, G. W., and Uhlenbeck, O. C. (1987) *Nucleic Acids Res. 15*, 8783−8789.

39. Darzynkiewicz, E., Stepinski, J., Ekiel, I., Jin, Y., Haber, D., Sijuwade, T., and Tahara, S. M. (1988) *Nucleic Acids Res. 16*, 8953−8960.
40. Merril, C. R., Goldman, D. Sedman, S. A., and Ebert, M. H. (1981) *Science 211*, 1437−1438.
41. Merril, C. R., Goldman, D., and van Keuren, M. L. (1982) *Electrophoresis 3*, 17−23.
42. Berry, M. J., and Samoel, C. E. (1982) *Anal. Biochem. 124*, 180−184.
43. Lakowicz, J. R. (1983) *Principle of Fluorescence Spectroscopy*, Chapter 10, Plenum Press, New York.
44. Heyduk, T., and Lee, J. C. (1990) *Proc. Natl. Acad. Sci. U.S.A. 87*, 1744−1748.
45. Matson, S. W., and Kaaiser-Rogus, K. A. (1990) *Annu. Rev. Biochem. 59*, 289−329.
46. Claude, A., Arenas, J., and Hurwitz, J. (1991) *J. Biol. Chem. 266*, 10358−10367.
47. Hiratsuka, T., and Uchida, K. (1973) *Arch. Biochem. Biophys. 320*, 635−647.
48. Hiratsuka, T. (1983) *Biochim. Biophys. Acta 742*, 496−508.
49. Hiratsuka, T. (1984) *J. Biochem. 96*, 155−162.
50. Bujialowski, W., and Klonowska, M. M. (1994) *Biochemistry 33*, 4682−4694.
51. Sha, M., Balasta, M. L., and Goss, D. J. (1994) *J. Biol. Chem. 269*, 14872−14877.
52. Seal, S. N., Schmidt, A., and Marcus, A. (1983) *Proc. Natl. Acad. Sci. U.S.A. 80*, 6562−6565.
53. Biswas, E. E., Biswas, B., and Bishop, J. E. (1986) *Biochemistry 25*, 7368−7374.
54. Volkenstein, M. V., and Goldstein, B. N. (1966) *Biochim. Biophys. Acta 115*, 471−477.
55. Abramson, R. D., Dever, T. E., and Merrick, W. C. (1988) *J. Biol. Chem. 263*, 6016−6019.
56. Mills, D. A., and Richter, M. L. (1991) *J. Biol. Chem. 266*, 7440−7444.

BI992322P